
Sufficient Invariant Learning for Distribution Shift

Taero Kim

Department of Statistics and Data Science
Yonsei University
taero.kim@yonsei.ac.kr

Sungjun Lim

Department of Artificial Intelligence
University of Seoul
lsj9862@uos.ac.kr

Kyungwoo Song*

Department of Applied Statistics
Department of Statistics and Data Science
Yonsei University
kyungwoo.song@yonsei.ac.kr

Abstract

Machine learning algorithms have shown remarkable performance in diverse applications. However, it is still challenging to guarantee performance in distribution shifts when distributions of training and test datasets are different. There have been several approaches to improve the performance in distribution shift cases by learning invariant features across groups or domains. However, we observe that the previous works only learn invariant features partially. While the prior works focus on the limited invariant features, we first raise the importance of the *sufficient* invariant features. Since only training sets are given empirically, the learned partial invariant features from training sets might not be present in the test sets under distribution shift. Therefore, the performance improvement on distribution shifts might be limited. In this paper, we argue that learning sufficient invariant features from the training set is crucial for the distribution shift case. Concretely, we newly observe the connection between a) sufficient invariant features and b) flatness differences between groups or domains. Moreover, we propose a new algorithm, Adaptive Sharpness-aware Group Distributionally Robust Optimization (ASGDRO), to learn sufficient invariant features across domains or groups. ASGDRO learns sufficient invariant features by seeking common flat minima across all groups or domains. Therefore, ASGDRO improves the performance on diverse distribution shift cases. Besides, we provide a new simple dataset, Heterogeneous-CMNIST, to diagnose whether the various algorithms learn sufficient invariant features.

1 Introduction

Generally, machine learning algorithms assume that the training distribution and test distribution are drawn from the same distribution. Under this identically and independently distributed (IID) assumption, machine learning algorithms have shown significant performance improvements in diverse domains. However, in the real-world, this assumption does not hold, and distribution shifts, where the training and test distribution differ, occur frequently. In such scenarios, machine learning algorithms often exhibit significant deterioration of generalization performance on the shifted test distribution. Therefore, developing robust models that can handle the distribution shift is a key challenge in the field of machine learning [12, 19, 32, 39].

*Corresponding Author

One of the main difficulties of distribution shift is spurious correlation, which appears to describe the class well in the training distribution but fails to do so in the test distribution. The strong correlation between class and spurious features in the training set hinders the model from learning invariant features that describe their classes well and regardless of distribution shifts [2, 30]. In subpopulation shift [32, 39], for example, practitioners aim to achieve balanced generalization performance across groups, represented by combinations of class and attribute. Spurious features serve as shortcuts for learning specific groups that dominate the training set, leading to the underrepresentation of groups comprised of relatively few data points [19, 40]. Furthermore, spurious correlation can degrade the generalization performance for unseen domains. By learning common invariant features among multiple training domains, we can improve domain generalization performance. However, spurious correlations that exert a strong influence on specific domains disturb the learning of these domain-invariant features in domain shift settings [12, 11].

As a result, research in invariant learning has been pursued to remove spurious correlation, thereby enhancing the model robustness in various distribution shift scenarios [6, 20, 34, 17].

However, even if our model successfully eliminates spurious correlations, the failure to learn a diverse set of invariant features could undermine its ability to guarantee generalization performance in the test domain. (Section 4.1). Specifically, if the invariant features learned by the model are absent in the test domain, the model will struggle to make accurate predictions under distribution shifts. As illustrated in Figure 1, a model that has learned a spurious feature performs poorly on shifted test samples. Despite using invariant learning algorithms to avoid learning spurious patterns, the model may still fail to capture a diverse set of features. For instance, a model that classifies ducks solely based on the shape of their webbed feet, yet fails to recognize a duck swimming in a pond as a duck. Therefore, building a robust model requires more than just eliminating spurious correlations; it also necessitates the learning of sufficiently diverse invariant features. We refer to this approach as *Sufficient Invariant Learning (SIL)*. Through SIL, we aim to train a model that is more robust to distribution shifts and guarantees enhanced generalization performance (Section 4).

One of the principal methods to improve generalization performance is to consider flatness. In IID setting, algorithms that take flatness into account have recently demonstrated superior performance in various tasks [10, 21, 16]. However, research considering flatness and its mechanism when spurious correlation exists is limited, and so far, it has been focused only on the domain shift situation [5, 42]. In this paper, we present for the first time that considering flatness in distribution shift scenarios enables the model to learn a sufficiently diverse set of invariant features (Section 3.1). Additionally, we argue that flatness is essential to lower the generalization gap in general distribution shift situations, not just in domain shifts but also in subpopulation shifts, where strong spurious correlations significantly corrupt the generalization performance of the conventional Empirical Risk Minimization (ERM) algorithm. To this end, we propose Adaptive Sharpness-aware Group Distributionally Robust Optimization (ASGDRO), which consistently achieves improved generalization performance in diverse distribution shifts scenarios by identifying the common flat minima for SIL (Section 3.2). We summarize our contributions as follows:

- We propose the necessity of SIL under distribution shift for the first time. Additionally, we argue that it is essential to find common flat minima across different groups or domains to achieve SIL.
- We propose ASGDRO, a SIL algorithm, designed to identify common flat minima. Moreover, we introduce a new dataset, Heterogeneous-CMNIST(H-CMNIST), which incorporates multiple invariant features along with spurious correlation, to demonstrate that ASGDRO is capable of learning a sufficiently diverse set of invariant features, unlike other invariant learning algorithms.
- We show the superior performance of ASGDRO across diverse distribution shifts. Using Grad-CAM and Hessian analysis, we show that ASGDRO achieves SIL and finds common flat minima.

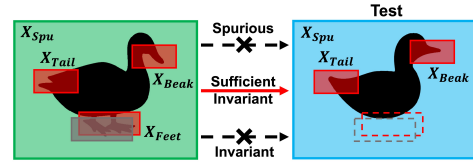


Figure 1: **Sufficient Invariant Learning** Left visualizes the image that contains spurious features, X_{Spu} , and multiple invariant features, X_{Tail} , X_{Beak} , and X_{Feet} in training set. If we focus on the X_{Spu} (green background), then we fail to predict correctly on the test set (right). Even if we capture the invariant features of the training set, X_{Feet} , we still fail to predict correctly when the invariant features are not present (gray). However, it is possible to predict correctly if we learn sufficiently diverse invariant features, X_{Feet} , X_{Tail} , and X_{Beak} . With sufficient invariant features, it is guaranteed to improve the performance even though some invariant features of the training set, X_{Feet} , are not present in the test set with remaining invariant features, X_{Tail} and X_{Beak} (red).

2 Relate Works

2.1 Invariant Learning for Distribution Shift

The standard approach to modern deep learning is Empirical Risk Minimization (ERM) [35], which minimizes the average training loss. However, ERM may not guarantee robustness in distribution shifts. To improve the generalization performance in distribution shift, Group Distributionally Robust Optimization (GDRO) minimizes worst-group loss for each step to alleviate learning spurious correlation [30]. Meanwhile, some studies utilize loss gradient for invariant learning. For example, Invariant Risk Minimization (IRM) minimizes the gradient norm of the fixed classifier across domains [2, 1]. Some research matches the loss gradient for each domain in order to find common invariant features [34, 29]. On the other hand, it is also possible to learn invariant features by conducting additional learning using re-weighting [25, 17], performing data augmentation through domain-specific mix-up [40]. However, such invariant learning algorithms may not guarantee sufficient invariant learning, and it is difficult to improve generalization performance. [12] shows that ERM achieves comparable domain generalization performance with other invariant learning algorithms under fair experimental conditions. In this paper, we demonstrate the necessity of learning invariant features sufficiently by showing the effective generalization performance of ASGDRO.

2.2 Flatness and Generalization

Many studies argue that finding flat minima is related to improving generalization performance [18, 28]. Based on this association, various algorithms have emerged to find flat minima. Sharpness-aware Minimization (SAM) finds flat minima by minimizing the maximum training loss of neighborhood within ρ radius on the parameter space [10]. Moreover, Adaptive SAM (ASAM) introduces the normalization operator to get a better correlation between flatness and generalization performance by avoiding the scale symmetries between the layers [21]. Stochastic Weight Averaging (SWA) also can reach the flat minima by averaging the weight repeatedly [16]. Research considering flatness in domain shift setting is also becoming a recent study [5, 42]. To the best of our knowledge, however, there is no research aimed at connecting flatness with a more general distribution shift situation, including subpopulation shift. It is also important for the model to perform robustly in the real-world, where various distribution shifts coexist in a complex manner with spurious correlation [19]. Therefore, we explain the relationship between flatness and SIL, demonstrating its efficacy across various distribution shifts.

3 Methodology

3.1 Flatness for Sufficient Invariant Learning

Before describing our methodology, we detail the necessity of flatness for SIL. GDRO is one of the representative invariant learning methods, and it minimizes the maximum loss across groups or domains¹:

$$L_{\text{GDRO}}(\theta) = \max_{g \in \mathbf{G}} L_g(\theta) = \max_{g \in \mathbf{G}} \mathbb{E}_{(\mathbf{x}_g, \mathbf{y}_g) \sim \hat{P}_g} l(\theta)$$

where \hat{P}_g stands for a group distribution in training set, L_g stands for ERM loss and \mathbf{G} refers to the set of group indices. GDRO successfully removes spurious correlation and learns invariant features [30]. However, after learning part of the invariant features, GDRO can fully minimize the training loss sufficiently by learning only the limited invariant features. To demonstrate this, we conduct a toy example. First, we assume that we know two parameters, θ_1^{inv} and θ_2^{inv} , in parameter space. Each parameter corresponds to a different invariant feature. That is, as we adjust θ_i^{inv} , the extent of corresponding invariant features used by the model for prediction changes. If the model successfully learns an invariant feature, it will have better generalization performance for that feature. In other words, for a well-learned invariant feature, the corresponding parameter θ_i^{inv} will have sufficiently low loss and flat minima [18, 16, 10].

¹In this paper, the terms 'group' and 'domain' will be used interchangeably

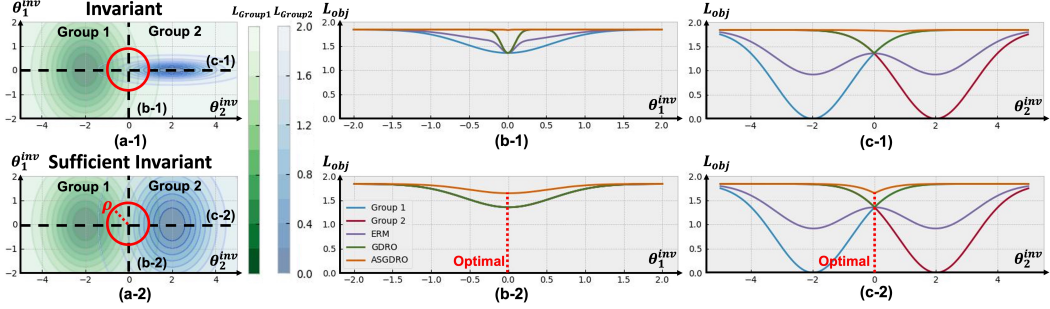


Figure 2: **Flatness for Sufficient Invariant Learning.** In (a-1) and (a-2), two axes, θ_1^{inv} and θ_2^{inv} , represent the parameters corresponding to each invariant features respectively. The red circle indicates the area bound by ρ when measuring flatness in ASGDRO. (b-1) and (b-2) show that when one direction, θ_1^{inv} , of Group 2 is sharp, GDRO still converges, but ASGDRO does not have any optimal point due to the sharpness of θ_1^{inv} . However, in (c-1) and (c-2) when both invariant directions of Group 2 as well as Group 1 are flat, ASGDRO has an optimal point and prefers to converge. That is, ASGDRO learns sufficient invariant features.

In a space composed of θ_1^{inv} and θ_2^{inv} , we aim to define the loss surface of each group. As a result, we also assume that the loss surface of each group follows a gaussian function of θ_1^{inv} and θ_2^{inv} :

$$f(\boldsymbol{\theta}) = \frac{1}{2\pi\sqrt{|\boldsymbol{\Sigma}|}} \exp\left(-\frac{1}{2}(\boldsymbol{\theta} - \boldsymbol{\mu})^T \boldsymbol{\Sigma}^{-1}(\boldsymbol{\theta} - \boldsymbol{\mu})\right)$$

$$\text{where } \boldsymbol{\theta} = \begin{bmatrix} \theta_1^{\text{inv}} \\ \theta_2^{\text{inv}} \end{bmatrix}, \boldsymbol{\mu} = \begin{bmatrix} \mu_1 \\ \mu_2 \end{bmatrix}, \boldsymbol{\Sigma} = \begin{bmatrix} \sigma_{11} & \sigma_{12} \\ \sigma_{21} & \sigma_{22} \end{bmatrix}.$$

To make the value greater than 0, we subtract $f(\boldsymbol{\theta})$ from its maximum value. As a result, we can define the loss surface corresponding to the two groups, each with a minimum value of 0, as follows:

$$\begin{aligned} L_{\text{Group1}}(\boldsymbol{\theta}) &= \max_{\boldsymbol{\theta}} f(\boldsymbol{\theta}; \boldsymbol{\mu}^{(1)}, \boldsymbol{\Sigma}^{(1)}) - f(\boldsymbol{\theta}; \boldsymbol{\mu}^{(1)}, \boldsymbol{\Sigma}^{(1)}) \\ L_{\text{Group2}}(\boldsymbol{\theta}) &= \max_{\boldsymbol{\theta}} f(\boldsymbol{\theta}; \boldsymbol{\mu}^{(2)}, \boldsymbol{\Sigma}^{(2)}) - f(\boldsymbol{\theta}; \boldsymbol{\mu}^{(2)}, \boldsymbol{\Sigma}^{(2)}) \end{aligned}$$

Now we can create sharp or flat minima in a specific direction by adjusting the covariance matrix $\boldsymbol{\Sigma}^{(i)}$. In this example, we consider a fixed situation where both Group 1 and Group 2 have flat minima with respect to θ_2^{inv} . When Group 1 always has flat minima with respect to θ_1^{inv} , our goal is to observe how the loss, L_{obj} , corresponding to each objective function, changes depending on whether Group 2 has sharp or flat minima with respect to θ_1^{inv} (a-1 and a-2 in Figure 2). The parameters that we use to generate the toy examples in Figure 2 are as follows:

$$\begin{aligned} \text{(a-1) Group 1: } \boldsymbol{\mu} &= \begin{bmatrix} -2.0 \\ 0.0 \end{bmatrix}, \boldsymbol{\Sigma} = \begin{bmatrix} 1.5 & 0.0 \\ 0.0 & 2.0 \end{bmatrix}, \quad \text{Group 2: } \boldsymbol{\mu} = \begin{bmatrix} 2.0 \\ 0.0 \end{bmatrix}, \boldsymbol{\Sigma} = \begin{bmatrix} 1.5 & 0.0 \\ 0.0 & 0.05 \end{bmatrix} \\ \text{(a-2) Group 1: } \boldsymbol{\mu} &= \begin{bmatrix} -2.0 \\ 0.0 \end{bmatrix}, \boldsymbol{\Sigma} = \begin{bmatrix} 1.5 & 0.0 \\ 0.0 & 2.0 \end{bmatrix}, \quad \text{Group 2: } \boldsymbol{\mu} = \begin{bmatrix} 2.0 \\ 0.0 \end{bmatrix}, \boldsymbol{\Sigma} = \begin{bmatrix} 1.5 & 0.0 \\ 0.0 & 2.0 \end{bmatrix}. \end{aligned}$$

For simplicity, we assume that the numbers of data points in the two groups are the same. For each parameter in the loss surface, we get the loss of ERM and GDRO as follows:

$$\begin{aligned} L_{\text{ERM}} &= (L_{\text{Group1}}(\boldsymbol{\theta}) + L_{\text{Group2}}(\boldsymbol{\theta}))/2 \\ L_{\text{GDRO}} &= \max \{L_{\text{Group1}}(\boldsymbol{\theta}), L_{\text{Group2}}(\boldsymbol{\theta})\} \end{aligned}$$

ASGDRO we propose in this paper is a methodology that considers flatness for SIL, and it can work as follows in this toy example in a simple way:

$$\begin{aligned} L_{\text{ASGDRO}} &= \max \{L_{\text{Group1}}(\boldsymbol{\theta} + \boldsymbol{\epsilon}^*), L_{\text{Group2}}(\boldsymbol{\theta} + \boldsymbol{\epsilon}^*)\} \\ \text{where } \boldsymbol{\epsilon}^* &= \underset{\|\boldsymbol{\epsilon}\| \leq \rho}{\text{argmax}} L_{\text{ERM}}(\boldsymbol{\theta} + \boldsymbol{\epsilon}) \end{aligned}$$

and ρ stands for the radius, or neighborhood size in the parameter space. The maximum value of the group loss among the groups at the parameter where the ERM loss is greatest within a circle with radius ρ is taken as the loss of ASGDRO. We use $\rho = 0.6$ in this example.

We can evaluate the loss surface in each direction in the parameter space through these objective functions (second and third columns of Figure 2). The situation where the loss surface of Group 2 is sharp for θ_1^{inv} (first row of Figure 2) can be considered as a situation where the invariant feature corresponding to θ_1^{inv} has not been sufficiently learned because the sharp minima cannot guarantee generalization performance [18, 16, 10]. However, GDRO, which has no regularization for flatness, only considers the loss at the current parameter and does not take into account the loss values at the neighborhood parameters. As a result, it may converge to a local minimum that learns limited invariant features, thus it cannot guarantee SIL. On the other hand, ASGDRO, which considers the loss of the neighborhood parameters, does not prefer parameters where θ_1^{inv} is sharp.

When the loss surface of Group 2 is flat for θ_1^{inv} (second row in Figure 2), we can say that the model performs SIL. GDRO, however, has the same loss at the optimal point in this situation as in the previous case, meaning that GDRO does not specifically regularize the model to perform SIL. On the other hand, ASGDRO has an optimal parameter point when θ_1^{inv} is flat, unlike before, and through this, we can say that flatness can regularize the model to sufficiently learn various invariant features. As a result, considering flatness, we can perform SIL and make more robust predictions in distribution shift settings, utilizing the multiple invariant features.

3.2 Adaptive Sharpness-aware Group Distributionally Robust Optimization

In the previous toy example, we demonstrated the relationship between flatness and SIL. We use the perturbation ϵ proposed in SAM [10] for the SIL algorithm that considers flatness.

$$L_{\text{SAM}} = \max_{\|\epsilon\| \leq \rho} L_{\mathbf{S}}(\boldsymbol{\theta} + \epsilon),$$

where ϵ stands for the random vectors whose ℓ_2 -norm are smaller than or equal to ρ . To find the adversarial perturbation ϵ^* , which is the approximation of the direction for the maximum loss in perturbation set $\{\boldsymbol{\theta} + \epsilon \mid \rho \geq \|\epsilon\|\}$, we use ERM loss, $L_{\mathbf{S}}(\boldsymbol{\theta})$. Fixing ϵ^* across groups using $L_{\mathbf{S}}$, we will find the group-invariant adversarial perturbation. That is, the approach to finding ϵ^* in our method shares the same step with SAM. Therefore, the adversarial perturbation is:

$$\epsilon^* = \underset{\|\epsilon\|_p \leq \rho}{\text{argmax}} L_{\mathbf{S}}(\boldsymbol{\theta} + \epsilon) = \rho \frac{\nabla_{\boldsymbol{\theta}} L_{\mathbf{S}}(\boldsymbol{\theta}_t)}{\|\nabla_{\boldsymbol{\theta}} L_{\mathbf{S}}(\boldsymbol{\theta}_t)\|} \quad \text{where} \quad L_{\mathbf{S}}(\boldsymbol{\theta}) = \mathbb{E}_{(\mathbf{x}, \mathbf{y}) \sim \hat{P}} l(\boldsymbol{\theta}; (\mathbf{x}, \mathbf{y})). \quad (1)$$

where \hat{P} stands for the distribution of the total training set. After ascending the parameter by adding ϵ^* , we get the group losses at the perturbed parameters and select the maximum group loss across groups. Therefore, our objective function is as follows:

$$\min_{\boldsymbol{\theta}} \max_{g \in \mathbf{G}} L_{\mathbf{S}}^g(\boldsymbol{\theta} + \epsilon^*).$$

Note that the adversarial perturbation ϵ^* is independent of the group information and the effects of fixed ϵ^* will be explained in Section 3.3.

We aim to achieve SIL through common flat minima across groups. However, in fact, the flat minima obtained through the adversarial perturbation of Equation 1 may not have a complete correlation with generalization performance due to the symmetries of the model [8]. This risk can be more fatal in the case of our current methodology, which aims to learn relatively underrepresented invariant features in the situation of distribution shift. Therefore, we increase the correlation between flatness and generalization by using ASAM [21], which has been proposed to solve scale symmetry. As a result, the modified algorithm is as follows, and we refer to this as Adaptive Sharpness-aware Group Distributionally Robust Optimization (ASGDRO):

$$L_{\text{ASGDRO}}(\boldsymbol{\theta}) = \max_{g \in \mathbf{G}} L_{\mathbf{S}}^g(\boldsymbol{\theta} + \epsilon^*), \quad \text{where} \quad \epsilon^* = \rho \frac{T_{\boldsymbol{\theta}_t}^2 \nabla_{\boldsymbol{\theta}} L_{\mathbf{S}}(\boldsymbol{\theta}_t)}{\|T_{\boldsymbol{\theta}_t} \nabla_{\boldsymbol{\theta}} L_{\mathbf{S}}(\boldsymbol{\theta}_t)\|}. \quad (2)$$

In equation 2, $T_{\boldsymbol{\theta}_t}$ is the element-wise or filter-wise normalization operator to correct the scale symmetries in a model. Finally, we update our model parameter from the original parameter:

$$\boldsymbol{\theta}_{t+1} = \boldsymbol{\theta}_t - \eta \nabla_{\boldsymbol{\theta}} L_{\mathbf{S}}^{g^*}(\boldsymbol{\theta}_t + \epsilon^*),$$

where g^* denotes the worst group which has the maximum group loss on the adversarial parameter.

Algorithm 1 ASGDRO

Input: Training dataset $\mathbf{S} = \{(\mathbf{x}_i, \mathbf{y}_i, g_i)\}$, Neighborhood radius $\rho > 0$, Learning rate $\eta > 0$, Robust step size $\gamma > 0$, The number of groups $|\mathbf{G}|$

- 1: Initialization: $\boldsymbol{\theta}_0$; $\lambda_0^g = 1/|\mathbf{G}|$, $g = 1 \dots |\mathbf{G}|$;
- 2: **for** $t = 1, 2, 3, \dots$ **do**
- 3: Compute training loss $L_{\mathbf{S}}(\boldsymbol{\theta}_t)$;
- 4: Compute $\boldsymbol{\epsilon}_t^* = \rho \frac{T_{\boldsymbol{\theta}_t}^2 \nabla L_{\mathbf{S}}(\boldsymbol{\theta}_t)}{\|T_{\boldsymbol{\theta}_t} \nabla L_{\mathbf{S}}(\boldsymbol{\theta}_t)\|}$;
- 5: Gradient ascent: $\boldsymbol{\theta}_t^* = \boldsymbol{\theta}_t + \boldsymbol{\epsilon}_t^*$;
- 6: Find each group loss $L_{\mathbf{S}}^g(\boldsymbol{\theta}_t^*)$;
- 7: Compute $\tilde{\lambda}_t^g = \lambda_{t-1}^g \exp(\gamma L_{\mathbf{S}}^g(\boldsymbol{\theta}_t^*))$ respectively;
- 8: Update $\lambda_t^g = \tilde{\lambda}_t^g / \sum_g \tilde{\lambda}_t^g$;
- 9: Compute $L_{\text{ASGDRO}}(\boldsymbol{\theta}_t) = \sum_g \lambda_t^g L_{\mathbf{S}}^g(\boldsymbol{\theta}_t^*)$;
- 10: Compute $\nabla_{\boldsymbol{\theta}_t} L_{\text{ASGDRO}}(\boldsymbol{\theta}_t) = \sum_g \lambda_t^g \nabla L_{\mathbf{S}}^g(\boldsymbol{\theta}_t)|_{\boldsymbol{\theta}_t^*}$;
- 11: Return to $\boldsymbol{\theta}_t$;
- 12: Update the parameters: $\boldsymbol{\theta}_{t+1} = \boldsymbol{\theta}_t - \eta \nabla L_{\text{ASGDRO}}(\boldsymbol{\theta}_t)$;
- 13: **end for**

3.3 Improved ASGDRO and Implementation

However, performing optimization with only selecting and minimizing the worst group causes the instability of convergence [30]. ASGDRO can also suffer from such instability. As a result, similar to GDRO, we adopt alternative gradient-based optimization algorithms. We can change ASGDRO objective into the form of linear interpolation and update their coefficients:

$$L_{\text{ASGDRO}}(\boldsymbol{\theta}) = \max_{g \in \mathbf{G}} L_{\mathbf{S}}^g(\boldsymbol{\theta} + \boldsymbol{\epsilon}^*) = \max_{\sum_g \lambda_g = 1, \lambda_g \geq 0} \sum_{g=1}^{|\mathbf{G}|} \lambda_g L_{\mathbf{S}}^g(\boldsymbol{\theta} + \boldsymbol{\epsilon}^*),$$

where λ_g is the weight imposed on each group loss updated at every step (Algorithm 1).

It is worth noting that we still find $\boldsymbol{\epsilon}^*$ using ERM loss for the training set regardless of the group information. If we use the group-specific adversarial perturbation $\boldsymbol{\epsilon}_g^*$, we have the following equation:

$$\max_{\sum_g \lambda_g = 1, \lambda_g \geq 0} \sum_{g=1}^{|\mathbf{G}|} \lambda_g L_{\mathbf{S}}^g(\boldsymbol{\theta} + \boldsymbol{\epsilon}_g^*).$$

This means that the position of the adversarial perturbation is different for each group. However, SAM is influenced by the size of the loss when comparing the flatness of two or more minima [44]. Especially since we are assuming distribution shift, there can be significantly different loss values for each group, and the instability of the flatness indicator increases. Incorrectly measured group flatness can overestimate or underestimate the coefficient λ_g as we can see in lines 7-9 of Algorithm 1. To make this more stable, it is important to find a fixed adversarial perturbation with the gradient obtained by the average loss, even in the situation of distribution shift, and to evaluate the flatness.

4 Results

4.1 ASGDRO Learns Sufficient Invariant Features

By finding the common flat minima, ASGDRO can learn sufficient invariant features. To demonstrate this, we propose Heterogeneous-CMNIST (H-CMNIST), a new dataset designed to evaluate whether the model learns sufficient invariant representation (Figure 3). More concretely, evaluating the model on H-CMNIST is to check whether the remaining invariant feature is additionally learned by the algorithm, assuming that the model has already learned one invariant feature.

H-CMNIST includes two invariant features, the color and shape of digits, and one spurious feature, the white box position (BP). Unlike Colored MNIST (CMNIST) [2], there is no injection of label noise. Each class has its own color and shape, so these features act as invariant features. BP consists of two attributes, Top Left and Bottom Right. This simplifies the typical situations where spurious features occur [30, 7]. Specifically, in the training set, 95% of the samples with Top Left BP belong to class 0,

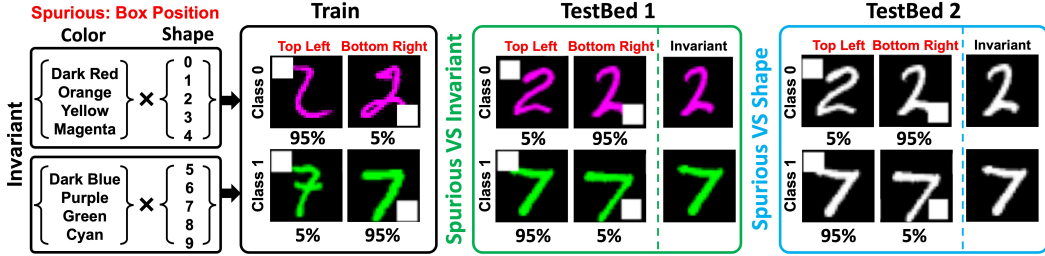


Figure 3: **Overview of H-CMNIST.** There are three kinds of features, color and shape for invariant features and box position for spurious feature. The ratio of the spurious feature is flipped between the train and test set. The test set consists of two testbeds, one for evaluating whether learning invariant features and the other for evaluating whether sufficient invariant features.

while only 5% belong to class 1. Conversely, 95% of the samples with Bottom Right BP are in class 1, with only 5% in class 0. Using this training set, we train various algorithms and evaluate their performance on multiple test sets. In all test sets, the ratio of BP is reversed compared to the training set: 95% of the samples with Bottom Right BP and 5% with Top Left BP are in class 0, and 95% with Top Left BP and 5% with Bottom Right BP are in class 1. As a result, models that strongly learn spurious correlations perform poorly on the test set. We construct two tests. TestBed 1 examines the performance differences based on the presence or absence of the spurious feature BP when both invariant features, color and shape, coexist. TestBed 2 observes the performance differences due to the spurious feature when only the invariant feature of shape is present. In other words, we create scenarios where some of the invariant features present in the training set are absent in the test set. For more details of the experiment setting, refer to Appendix B.

Table 1 shows the results of H-CMNIST. First, we conduct TestBed 1, which is to evaluate whether the model learns successfully invariant features, color or shape, when an existing spurious feature, BP. All baseline models, including ASGDRO, successfully learn invariant features despite the existence of spurious features and the performance does not change significantly depending on the presence or absence of spurious features. In other words, every model successfully captures at least one of the invariant features. Additionally, the successful learning of invariant features in all algorithms, despite the presence of spurious features, indicates that invariant correlation is acting more strongly than spurious correlation. This reflects well the situation where we have assumed that invariant learning has already been successfully performed in H-CMNIST.

However, the results from Testbed 1 do not guarantee SIL. When conducting tests on Testbed 2, where we exclude the color invariant feature, both ERM and ASAM show significant performance differences depending on the presence of spurious features. With the results of two Testbeds, we can say that ERM and ASAM only learn color invariant feature successfully but they fail to capture additional invariant features, shape, beating the spurious correlation for prediction. This means that successfully removing spurious correlation to create a so-called robust model does not guarantee that it has learned sufficiently diverse invariant features. Therefore, it is important to learn sufficient invariant representation for the robustness of the model.

Existing invariant learning algorithms also struggle to learn additional invariant features. GDRO exhibits robustness to spurious correlations for prediction using shape features compared to ERM and ASAM in Testbed 2. However, when only the shape feature is provided, GDRO shows only marginal improvement. We can infer that this is because of its prior learning of color invariant feature, as we also mentioned in Section 3.1. However, ASGDRO not only eliminates spurious correlations but also exhibits more successful prediction with respect to shape, compared to other baselines. ASGDRO optimizes the model to learn invariant features considering their flatness; therefore, it can achieve SIL even on distribution shift settings. In other words, by pursuing the common flat minima, one can prevent the learning of limited invariant features and ensure the learning of sufficiently diverse invariant features.

Table 1: **Results of H-CMNIST.** H-CMNIST consists

of two test beds. TestBed 1 shows which representation the model primarily learned between spurious and invariant features. TestBed 2, on the other hand, check which model learn sufficient invariant feature, that is, not only color but also shape by evaluating the model when only the shape is given for the invariant feature.

Table 1 shows the results of H-CMNIST. First, we conduct TestBed 1, which is to evaluate whether the model learns successfully invariant features, color or shape, when an existing spurious feature, BP. All baseline models, including ASGDRO, successfully learn invariant features despite the existence of spurious features and the performance does not change significantly depending on the presence or absence of spurious features. In other words, every model successfully captures at least one of the invariant features. Additionally, the successful learning of invariant features in all algorithms, despite the presence of spurious features, indicates that invariant correlation is acting more strongly than spurious correlation. This reflects well the situation where we have assumed that invariant learning has already been successfully performed in H-CMNIST.

However, the results from Testbed 1 do not guarantee SIL. When conducting tests on Testbed 2, where we exclude the color invariant feature, both ERM and ASAM show significant performance differences depending on the presence of spurious features. With the results of two Testbeds, we can say that ERM and ASAM only learn color invariant feature successfully but they fail to capture additional invariant features, shape, beating the spurious correlation for prediction. This means that successfully removing spurious correlation to create a so-called robust model does not guarantee that it has learned sufficiently diverse invariant features. Therefore, it is important to learn sufficient invariant representation for the robustness of the model.

Existing invariant learning algorithms also struggle to learn additional invariant features. GDRO exhibits robustness to spurious correlations for prediction using shape features compared to ERM and ASAM in Testbed 2. However, when only the shape feature is provided, GDRO shows only marginal improvement. We can infer that this is because of its prior learning of color invariant feature, as we also mentioned in Section 3.1. However, ASGDRO not only eliminates spurious correlations but also exhibits more successful prediction with respect to shape, compared to other baselines. ASGDRO optimizes the model to learn invariant features considering their flatness; therefore, it can achieve SIL even on distribution shift settings. In other words, by pursuing the common flat minima, one can prevent the learning of limited invariant features and ensure the learning of sufficiently diverse invariant features.

	CMNIST		Waterbirds		CelebA		CivilComments		Multi-NLI	
	Avg	Worst	Avg	Worst	Avg	Worst	Avg	Worst	Avg	Worst
ERM [†]	27.8%	0.0%	97.0%	63.7%	94.9%	47.8%	92.2%	56.0%	82.4%	67.9%
ASAM	40.5%	34.1%	97.4%	72.4%	93.6%	43.3%	92.6%	61.6%	82.2%	68.6%
IRM [†]	72.1%	70.3%	87.5%	75.6%	94.0%	77.8%	88.8%	66.3%	-	-
IB-IRM [†]	72.2%	70.7%	88.5%	76.5%	93.6%	85.0%	89.1%	65.3%	-	-
V-REx [†]	71.7%	70.2%	88.0%	73.6%	92.2%	86.7%	90.2%	64.9%	-	-
CORAL [†]	71.8%	69.5%	90.3%	79.8%	93.8%	76.9%	88.7%	65.6%	-	-
GDRO [†]	72.3%	68.6%	91.8%	90.6%	92.1%	87.2%	89.9%	70.0%	81.4%	77.7%
DomainMix [†]	51.4%	48.0%	76.4%	53.0%	93.4%	65.6%	90.9%	63.6%	-	-
Fish [†]	46.9%	35.6%	85.6%	64.0%	93.1%	61.2%	89.8%	71.1%	-	-
LISA [†]	74.0%	73.3%	91.8%	89.2%	92.4%	89.3%	89.2%	72.6%	-	-
ASGDRO	74.8%	74.2%	92.6%	91.0%	92.9%	90.0%	90.2%	71.4%	81.4%	79.0%

Table 2: **Subpopulation Shift.** ASGDRO consistently shows superior performance on worst group accuracy. Besides, ASGDRO also shows the best average performance on CMNIST and comparable performance on all dataset. [†] denotes the performance reported from [40, 25].

Model selection: training-domain validation set					
Algorithm	VLCS	PACS	OffHome	Terrainc	
ResNet18 [†]	73.2 ± 0.9	80.3 ± 0.4	55.7 ± 0.2	40.7 ± 0.3	62.5
ResNet50 [†]	75.5 ± 0.1	83.9 ± 0.2	64.4 ± 0.2	45.4 ± 1.2	67.3
Mixer-L16 [†]	76.4 ± 0.2	81.3 ± 1.0	69.4 ± 1.6	37.1 ± 0.4	66.1
BiT-M-R50x3 [†]	76.7 ± 0.1	84.4 ± 1.2	69.2 ± 0.6	52.5 ± 0.3	70.7
BiT-M-R101x3 [†]	75.0 ± 0.6	84.0 ± 0.7	67.7 ± 0.5	47.8 ± 0.8	68.6
BiT-M-R152x2 [†]	76.7 ± 0.3	85.2 ± 0.1	71.3 ± 0.6	51.4 ± 0.6	71.1
ViT-B16 [†]	79.2 ± 0.3	85.7 ± 0.1	78.4 ± 0.3	41.8 ± 0.6	71.3
ViT-L16 [†]	78.2 ± 0.5	84.6 ± 0.5	78.0 ± 0.1	42.7 ± 1.9	70.9
DeiT [†]	79.3 ± 0.4	87.8 ± 0.5	76.6 ± 0.3	50.0 ± 0.2	73.4
HViT [†]	79.2 ± 0.5	89.7 ± 0.4	80.0 ± 0.2	51.4 ± 0.9	75.1
DPLCLIP	80.8 ± 1.1	96.1 ± 0.2	82.3 ± 0.2	43.9 ± 1.2	75.8
DPLCLIP GDRO	80.3 ± 0.8	95.7 ± 0.3	82.9 ± 0.5	43.4 ± 1.3	75.6
DPLCLIP ASGDRO	82.2 ± 0.6	96.6 ± 0.3	83.5 ± 0.1	47.6 ± 0.8	77.5

Table 3: **Performance on DomainBed** Accuracy on DomainBed test dataset. [†] denotes the performance reported in [15]. All experiments except [†] are conducted following the DomainBed experimental settings [12].

4.2 Subpopulation Shift

We conduct experiments for subpopulation shift with diverse datasets, CMNIST [2], Waterbirds [30], CelebA [26], CivilComments [4] and Multi-NLI [38]. Detailed information about the dataset and hyperparameter tuning range can be found in the Appendix. The main purpose of the subpopulation shift task is to obtain the better worst group performance by learning invariant features. Unlike H-CMNIST, the spurious correlations act as stronger shortcuts in these datasets. As a result, the models cannot learn any invariant feature easily.

Table 2 shows the results of subpopulation shift experiments. ASGDRO shows the best worst-group performance for all data except CivilComments. For CivilComments data, ASGDRO also shows comparable performance with the best algorithms among the baselines. Moreover, ASGDRO decreases the gap between the average accuracy and the worst group accuracy compared with GDRO which is the most similar algorithm with ASGDRO, except Waterbirds. It means that ASGDRO effectively removed the spurious correlation while learning the diverse invariant feature that can work well across different groups. As a result, the results from the subpopulation shift experiment, along with the experiments in H-CMNIST, provide support for our claim that flatness can make SIL and ASGDRO learn sufficient invariant features.

4.3 Domain Shifts: DomainBed Benchmark

In domain shift setting, the main purpose is to learn common invariant features among the diverse represented domains to generalize well on the unseen domain. We can improve the domain generalization performance by removing the spurious correlation for a specific domain and learning diverse common features. As ASGDRO finds the common flat minima and learns sufficient invariant features,

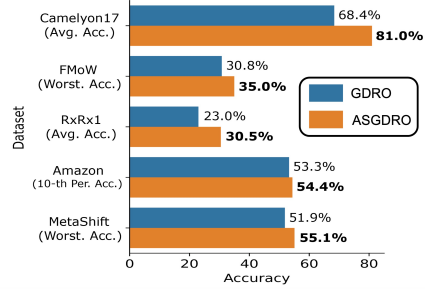


Figure 4: **Comparsion between GDRO and ASGDRO on Wilds Benchmark and MetaShift.** ASGDRO outperforms GDRO consistently.



Figure 5: **Grad-Cam Results** Landbird on land and waterbird on water are majority groups and landbird on water waterbird on land are minority. ASGDRO finds sufficient invariant features (the overall shape of birds).

it also work well in domain shift. We conducted DomainBed benchmark [12], which is the most commonly used benchmark for evaluating domain generalization performance under a fair setting.

ASGDRO is a model-agnostic method and can be easily applied to various algorithms. Therefore, it can be readily combined with the state-of-the-art (SOTA) models and contribute to further performance enhancement. We apply ASGDRO with DPLCLIP [41] which performs the prompt tuning for domain generalization and is the SOTA model on OfficeHome dataset [36] in the transfer learning setting. Table 2 shows that ASGDRO shows better performance in all datasets compared to DPLCLIP. ASGDRO also achieved better performance compared to the algorithm that combined DPLCLIP and GDRO. This means that SIL, considering flatness, is also effective in the situation of domain shift. In Appendix D, we have detailed the experimental settings and reported the performance for each domain across various datasets.

4.4 Distribution Shifts in Real-world

Distribution shifts occur more frequently and in more complex forms in real-world. These complicated forms of distribution shift represent a significant challenge that machine learning algorithms should overcome to be effectively used in the real-world. Wilds Benchmark [19] is for evaluating models, including datasets not only under domain shift, Camelyon17 and RxRx1, and subpopulation shift, CivilComments, but also a combination of domain and subpopulation shift, Amazon and FMoW based on real-world data. We have already conducted the experiment for CivilComments which is in subpopulation shift (Section 4.2), we instead perform the experiment for MetaShift [24] as in [40].

Figure 4 shows the results of ASGDRO and GDRO on Wilds Benchmark and MetaShift dataset. ASGDRO shows better performances, compared to GDRO throughout all datasets consistently. This demonstrates that SIL is important for real-world datasets as well, and that finding common flat minima boosts the generalization performance of existing invariant learning algorithms like GDRO. In other words, even if some of the invariant features we have learned do not exist in the test domain, if the learned invariant feature set is diversely composed, it ensures more robust predictions for the real world. As a result, this leads to significant performance improvement compared to the invariant learning algorithm, GDRO, which only learns a limited subset of invariant features.

4.5 Visual Interpretation by Grad-CAM

We conduct Grad-CAM analysis [33] to verify whether the effect of learning sufficient invariant features is being properly applied on the ground-truth label. In Waterbirds, minority groups, landbird on water and waterbird on land, can be underrepresented by the spurious correlation as they have only a few samples. In Figure 5, ERM and ASAM use various invariant features for prediction for majority groups, landbird on land and waterbird on water, but fail to remove spurious correlation, so we can see that they also use the feature of background. However, for the minority groups, only a small part of the invariant features is observed to be used for prediction. In other words, the invariant features of the majority and minority groups are the same, but the areas of the image that the model focuses on differ greatly due to the differences in the spurious feature, the background. This shows that ERM and ASAM are not performing invariant learning.

GDRO successfully removes spurious correlation regardless of the group. However, it uses only part of the invariant features for prediction, as previously discussed in Section 3.1. On the other hand, ASGDRO focuses on various invariant features for prediction regardless of the group. That is, ASGDRO focuses on the overall invariant features of waterbird and landbird. Additionally, ASGDRO successfully excludes spurious features in their prediction. In other words, we can achieve sufficient

Method	The Largest Eigenvalue			The Second Largest Eigenvalue		
	Majority	Minority	Total	Majority	Minority	Total
ERM	990	4894	2265	166	511	709
ASAM	972	5475	2624	178	524	647
GDRO	131	447	353	118	346	129
ASGDRO	107	342	279	98	274	105

Table 4: Hessian Analysis on Waterbirds Dataset. We present the largest eigenvalue and second largest eigenvalue for the Hessian of each model. ERM and ASAM show significant sharpness, especially in the worst groups. GDRO also finds flat minima relative to ERM and ASAM, however, ASGDRO finds flatter minima for every group than GDRO. That is, ASGDRO finds better common flat minima compared with GDRO

invariant learning by considering flatness using ASGDRO. For additional results on Grad-CAM, please refer to the Appendix C.

4.6 Hessian Analysis

We demonstrate that ASGDRO can find the common flat minima. We use the eigenvalue of Hessian to quantitatively measure and compare the flatness of the model. In Table 4, ERM and ASAM have significantly sharper minima for the worst group compared to GDRO and ASGDRO due to the spurious correlation, although ASAM is designed to find flat minima. Compared to GDRO and other baselines, ASGDRO achieves the lowest eigenvalue on the first and second maximum eigenvalue for every group. In particular, ASGDRO shows a large decrease in eigenvalues for the worst groups compared to their baselines. Moreover, in Figure 6, while GDRO fails to find the common flat minima across all groups, ASGDRO finds parameters with similar flatness for all groups. Additionally, compared to GDRO, it ensures a flatter minima for each group. Therefore, we can conclude that ASGDRO can find the common flat minima successfully.

5 Conclusion

In this paper, we point out the importance of SIL, which ensures better generalization ability in distribution shift by learning the sufficiently diverse invariant features. Through the newly introduced H-CMNIST dataset, we demonstrate that existing invariant learning algorithms learn only the part of invariant features. This indicates that if the learned invariant feature does not exist in the test domain, it still fails to ensure generalization performance. Therefore, we highlight that the model should learn sufficiently diverse set of invariant features for robust prediction. We also show that considering flatness encourages SIL and propose ASGDRO to find common flat minima in distribution shift settings. ASGDRO shows consistent performance in various and complex forms of distribution shift situations. Additionally, through Hessian analysis, we qualitatively analyzed whether ASGDRO actually exhibits common flat minima, and ultimately demonstrated, through empirical results using GradCAM, that flatness encourages the ability to perform SIL.

References

- [1] Kartik Ahuja, Ethan Caballero, Dinghuai Zhang, Jean-Christophe Gagnon-Audet, Yoshua Bengio, Ioannis Mitliagkas, and Irina Rish. Invariance principle meets information bottleneck for out-of-distribution generalization. *Advances in Neural Information Processing Systems*, 34:3438–3450, 2021.
- [2] Martin Arjovsky, Léon Bottou, Ishaaan Gulrajani, and David Lopez-Paz. Invariant risk minimization. *arXiv preprint arXiv:1907.02893*, 2019.
- [3] Sara Beery, Grant Van Horn, and Pietro Perona. Recognition in terra incognita. In *Proceedings of the European conference on computer vision (ECCV)*, pages 456–473, 2018.

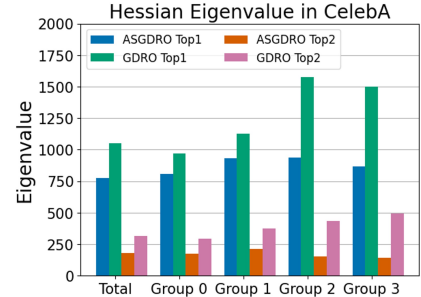


Figure 6: Hessian Analysis on CelebA Dataset. ASGDRO successfully finds the common flat minima across all groups.

- [4] Daniel Borkan, Lucas Dixon, Jeffrey Sorensen, Nithum Thain, and Lucy Vasserman. Nuanced metrics for measuring unintended bias with real data for text classification. In *Companion proceedings of the 2019 world wide web conference*, pages 491–500, 2019.
- [5] Junbum Cha, Sanghyuk Chun, Kyungjae Lee, Han-Cheol Cho, Seunghyun Park, Yunsung Lee, and Sungrae Park. Swad: Domain generalization by seeking flat minima. *Advances in Neural Information Processing Systems*, 34:22405–22418, 2021.
- [6] Elliot Creager, Jörn-Henrik Jacobsen, and Richard Zemel. Environment inference for invariant learning. In *International Conference on Machine Learning*, pages 2189–2200. PMLR, 2021.
- [7] Alex J DeGrave, Joseph D Janizek, and Su-In Lee. Ai for radiographic covid-19 detection selects shortcuts over signal. *Nature Machine Intelligence*, 3(7):610–619, 2021.
- [8] Laurent Dinh, Razvan Pascanu, Samy Bengio, and Yoshua Bengio. Sharp minima can generalize for deep nets. *CoRR*, abs/1703.04933, 2017.
- [9] Chen Fang, Ye Xu, and Daniel N Rockmore. Unbiased metric learning: On the utilization of multiple datasets and web images for softening bias. In *Proceedings of the IEEE International Conference on Computer Vision*, pages 1657–1664, 2013.
- [10] Pierre Foret, Ariel Kleiner, Hossein Mobahi, and Behnam Neyshabur. Sharpness-aware minimization for efficiently improving generalization. In *International Conference on Learning Representations*, 2020.
- [11] Irena Gao, Shiori Sagawa, Pang Wei Koh, Tatsunori Hashimoto, and Percy Liang. Out-of-domain robustness via targeted augmentations. *arXiv preprint arXiv:2302.11861*, 2023.
- [12] Ishaan Gulrajani and David Lopez-Paz. In search of lost domain generalization. *arXiv preprint arXiv:2007.01434*, 2020.
- [13] Zongbo Han, Zhipeng Liang, Fan Yang, Liu Liu, Lanqing Li, Yatao Bian, Peilin Zhao, Bingzhe Wu, Changqing Zhang, and Jianhua Yao. Umix: Improving importance weighting for subpopulation shift via uncertainty-aware mixup. *arXiv preprint arXiv:2209.08928*, 2022.
- [14] Kaiming He, Xiangyu Zhang, Shaoqing Ren, and Jian Sun. Deep residual learning for image recognition. In *Proceedings of the IEEE conference on computer vision and pattern recognition*, pages 770–778, 2016.
- [15] Yusuke Iwasawa and Yutaka Matsuo. Test-time classifier adjustment module for model-agnostic domain generalization. *Advances in Neural Information Processing Systems*, 34:2427–2440, 2021.
- [16] P Izmailov, AG Wilson, D Podoprikin, D Vetrov, and T Garipov. Averaging weights leads to wider optima and better generalization. In *34th Conference on Uncertainty in Artificial Intelligence 2018, UAI 2018*, pages 876–885, 2018.
- [17] Pavel Izmailov, Polina Kirichenko, Nate Gruver, and Andrew G Wilson. On feature learning in the presence of spurious correlations. *Advances in Neural Information Processing Systems*, 35:38516–38532, 2022.
- [18] Nitish Shirish Keskar, Dheevatsa Mudigere, Jorge Nocedal, Mikhail Smelyanskiy, and Ping Tak Peter Tang. On large-batch training for deep learning: Generalization gap and sharp minima. *arXiv preprint arXiv:1609.04836*, 2016.
- [19] Pang Wei Koh, Shiori Sagawa, Henrik Marklund, Sang Michael Xie, Marvin Zhang, Akshay Balsubramani, Weihua Hu, Michihiro Yasunaga, Richard Lanas Phillips, Irena Gao, et al. Wilds: A benchmark of in-the-wild distribution shifts. In *International Conference on Machine Learning*, pages 5637–5664. PMLR, 2021.
- [20] David Krueger, Ethan Caballero, Joern-Henrik Jacobsen, Amy Zhang, Jonathan Binas, Dinghuai Zhang, Remi Le Priol, and Aaron Courville. Out-of-distribution generalization via risk extrapolation (rex). In *International Conference on Machine Learning*, pages 5815–5826. PMLR, 2021.
- [21] Jungmin Kwon, Jeongseop Kim, Hyunseo Park, and In Kwon Choi. Asam: Adaptive sharpness-aware minimization for scale-invariant learning of deep neural networks. In *International Conference on Machine Learning*, pages 5905–5914. PMLR, 2021.
- [22] Yann LeCun, Léon Bottou, Yoshua Bengio, and Patrick Haffner. Gradient-based learning applied to document recognition. *Proceedings of the IEEE*, 86(11):2278–2324, 1998.

[23] Da Li, Yongxin Yang, Yi-Zhe Song, and Timothy M Hospedales. Deeper, broader and artier domain generalization. In *Proceedings of the IEEE international conference on computer vision*, pages 5542–5550, 2017.

[24] Weixin Liang and James Zou. Metashift: A dataset of datasets for evaluating contextual distribution shifts and training conflicts. *arXiv preprint arXiv:2202.06523*, 2022.

[25] Evan Z Liu, Behzad Haghgoo, Annie S Chen, Aditi Raghunathan, Pang Wei Koh, Shiori Sagawa, Percy Liang, and Chelsea Finn. Just train twice: Improving group robustness without training group information. In *International Conference on Machine Learning*, pages 6781–6792. PMLR, 2021.

[26] Ziwei Liu, Ping Luo, Xiaogang Wang, and Xiaoou Tang. Deep learning face attributes in the wild. In *Proceedings of the IEEE international conference on computer vision*, pages 3730–3738, 2015.

[27] Ilya Loshchilov and Frank Hutter. Decoupled weight decay regularization. *arXiv preprint arXiv:1711.05101*, 2017.

[28] Behnam Neyshabur, Srinadh Bhojanapalli, David McAllester, and Nati Srebro. Exploring generalization in deep learning. *Advances in neural information processing systems*, 30, 2017.

[29] Alexandre Rame, Corentin Dancette, and Matthieu Cord. Fishr: Invariant gradient variances for out-of-distribution generalization. In *International Conference on Machine Learning*, pages 18347–18377. PMLR, 2022.

[30] Shiori Sagawa, Pang Wei Koh, Tatsunori B Hashimoto, and Percy Liang. Distributionally robust neural networks. In *International Conference on Learning Representations*, 2019.

[31] Victor Sanh, Lysandre Debut, Julien Chaumond, and Thomas Wolf. Distilbert, a distilled version of bert: smaller, faster, cheaper and lighter. *arXiv preprint arXiv:1910.01108*, 2019.

[32] Shibani Santurkar, Dimitris Tsipras, and Aleksander Madry. Breeds: Benchmarks for subpopulation shift. *arXiv preprint arXiv:2008.04859*, 2020.

[33] Ramprasaath R. Selvaraju, Michael Cogswell, Abhishek Das, Ramakrishna Vedantam, Devi Parikh, and Dhruv Batra. Grad-cam: Visual explanations from deep networks via gradient-based localization. In *2017 IEEE International Conference on Computer Vision (ICCV)*, pages 618–626, 2017.

[34] Yuge Shi, Jeffrey Seely, Philip HS Torr, N Siddharth, Awni Hannun, Nicolas Usunier, and Gabriel Synnaeve. Gradient matching for domain generalization. *arXiv preprint arXiv:2104.09937*, 2021.

[35] Vladimir Vapnik. *The nature of statistical learning theory*. Springer science & business media, 1999.

[36] Hemanth Venkateswara, Jose Eusebio, Shayok Chakraborty, and Sethuraman Panchanathan. Deep hashing network for unsupervised domain adaptation. In *Proceedings of the IEEE conference on computer vision and pattern recognition*, pages 5018–5027, 2017.

[37] Catherine Wah, Steve Branson, Peter Welinder, Pietro Perona, and Serge Belongie. The caltech-ucsd birds-200-2011 dataset. 2011.

[38] Adina Williams, Nikita Nangia, and Samuel R Bowman. A broad-coverage challenge corpus for sentence understanding through inference. *arXiv preprint arXiv:1704.05426*, 2017.

[39] Yuzhe Yang, Haoran Zhang, Dina Katabi, and Marzyeh Ghassemi. Change is hard: A closer look at subpopulation shift. *arXiv preprint arXiv:2302.12254*, 2023.

[40] Huaxiu Yao, Yu Wang, Sai Li, Linjun Zhang, Weixin Liang, James Zou, and Chelsea Finn. Improving out-of-distribution robustness via selective augmentation. In *International Conference on Machine Learning*, pages 25407–25437. PMLR, 2022.

[41] Xin Zhang, Yusuke Iwasawa, Yutaka Matsuo, and Shixiang Shane Gu. Amortized prompt: Lightweight fine-tuning for clip in domain generalization. *arXiv preprint arXiv:2111.12853*, 2021.

[42] Xingxuan Zhang, Renzhe Xu, Han Yu, Yancheng Dong, Pengfei Tian, and Peng Cu. Flatness-aware minimization for domain generalization. *arXiv preprint arXiv:2307.11108*, 2023.

- [43] Bolei Zhou, Agata Lapedriza, Aditya Khosla, Aude Oliva, and Antonio Torralba. Places: A 10 million image database for scene recognition. *IEEE transactions on pattern analysis and machine intelligence*, 40(6):1452–1464, 2017.
- [44] Juntang Zhuang, Boqing Gong, Liangzhe Yuan, Yin Cui, Hartwig Adam, Nicha C Dvornek, James s Duncan, Ting Liu, et al. Surrogate gap minimization improves sharpness-aware training. In *International Conference on Learning Representations*, 2021.

SUPPLEMENTARY MATERIALS

A Subpopulation Shifts: Datasets and Experimental Details

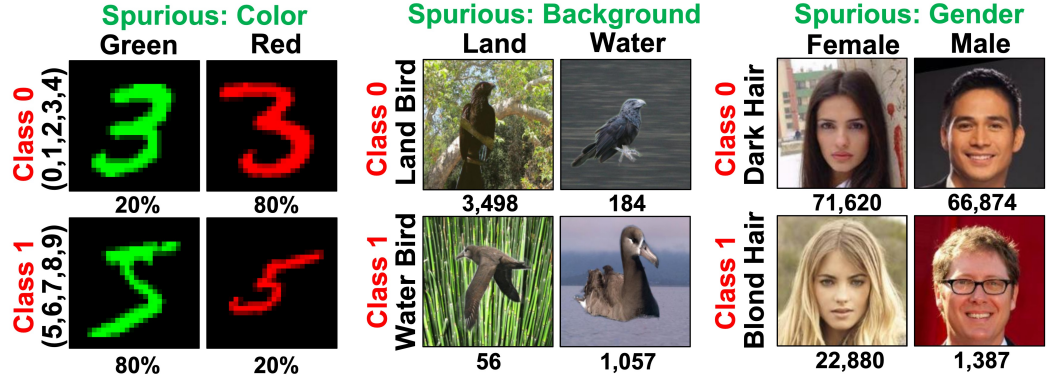


Figure 7: **Datasets for Computer Vision Tasks: CMNIST, Waterbirds, CelebA** In each dataset, each row represents the class and each column represents the spurious feature. The numbers written below the images represent the ratio or count of data belonging to each group in the training dataset, where each group consists of (Class, Spurious Feature) pairs.

In Table 2 of the main paper, we conducted our experiment for subpopulation shifts with five datasets; CMNIST [2], Waterbirds [30], CelebA [26], CivilComments [4], and Multi-NLI [38]. CMNIST, Waterbirds, and CelebA datasets correspond to computer vision tasks (Figure 7), while CivilComments and Multi-NLI pertain to natural language processing tasks. In this section, we will describe each dataset and provide experimental details. To implement this, we utilized the codes provided by [40]² for all datasets except for Multi-NLI [25]³.

A.1 Colored MNIST (CMNIST)

In the CMNIST dataset provided by [2], we perform binary classification to predict which number corresponds to the shape of a given digit. Specifically, when the shape of the digit corresponds to a logit between 0 and 4, the class is assigned as 0, and when it falls between 5 and 9, the class is assigned as 1. However, unlike the original MNIST dataset [22], CMNIST introduces color as a spurious feature in the training set. When this spurious correlation becomes stronger than the invariant relationship between the class and the shape of the digit, a model trained without any regularization may be prone to relying on the spurious feature for predictions.

While [2] constructed two environments with different ratios of spurious features in the training set, [40] used a single environment to compose the training set. Our CMNIST dataset experiment follows the same setting as [40], where the dataset consists of four groups when considering combinations of “Shape of Logit” and “Color” as a single group. Concretely, Class 0 and Class 1 have similar numbers of data points, but the distribution of spurious feature differs between the two classes. Class 0 consists of 80% red logits and 20% green logits, while Class 1 has 80% green logits and 20% red logits. Furthermore, within each class, 25% of the data acts as label noise, having a logit shape that does not correspond to its class. Therefore, the spurious feature, color, forms a stronger correlation between classes compared to that of the invariant feature, the shape of logits.

The validation set was constructed with an equal number of datapoint per group. The worst-group accuracy, defined as the lowest accuracy among all the groups, was utilized to select the best model. For the test set, we assume a distribution of the spurious feature that is opposite to the training set. Specifically, for Class 0, 90% of the data has a red color, and 10% has a green color, while for Class 1, it is the opposite. This is done to assess whether the model relies on the spurious feature for predictions.

²<https://github.com/huaxiuyao/LISA>

³<https://github.com/anniesch/jtt>

A.2 Waterbirds

Waterbirds dataset, constructed by [30], is designed for the task of determining whether a bird belongs to the Landbird or Waterbird class. It consists of images of birds, from [37], as the invariant feature, while the spurious feature is the background, from [43], which can either be Water or Land background. Indeed, in the Waterbirds dataset, the groups are formed by the combination of “Bird” and “Background”. Specifically, the bird images corresponding to each class consist of more than 10 different species of birds. On the other hand, each background is composed of two categories obtained from [43]. As can be seen in Figure 7, the Landbird class predominantly has images with Land background, while the majority of images in the Waterbird class have Water background. Therefore, the spurious feature, background, may indeed form a strong spurious correlation with each class.

We follow the setting of previous research, [30, 40], for the validation and test processes as well. The best model is selected based on the highest worst-group accuracy on the validation set. Unlike the training set, the validation and test sets are designed to have an equal number of images for each group within each class. When reporting the average accuracy on the test dataset using the best model, we first compute the group accuracy for each group in the test set. Then, we calculate the weighted average of these accuracies using the group distribution from the training set. This approach is adopted to mitigate the uncertainty in estimating group accuracies, as the number of images belonging to the minority group in the Waterbird dataset is significantly smaller compared to other datasets [30].

A.3 CelebA

CelebA dataset by [26] is a collection of facial images of celebrities from around the world. It includes attribute values associated with each individual, such as hair color, and gender. In order to evaluate the effects of subpopulation shifts, [30] reformulated the CelebA dataset to align with the task of predicting whether the hair color is blond or not. In this case, the spurious feature is gender, and thus, the dataset is composed of four groups based on the combinations of hair color and gender. It can be observed from Figure 7 that images belonging to Class 0, corresponding to dark hair rather, are plentiful regardless of gender. However, for images in Class 1, which represent blond hair, the majority of them are distributed in the Female group. Therefore, gender can act as a spurious feature, and the goal of this task is to obtain a model that focuses solely on the invariant feature, hair color, rather than the face which may capture the characteristics of gender-related features.

The best model is selected based on the highest worst-group accuracy on the validation set. In this case, the validation set and test set have the same distribution of images per group as the training set. Therefore, the average test accuracy reflects this distribution accordingly.

A.4 CivilComments

The CivilComments dataset, [4], is a dataset that gathers comments from online platforms and is used for the task of classifying whether a given comment is toxic or not. We conduct the experiment on the CivilComments dataset, which has been reformulated by [19]. Each comment is labeled to indicate whether it mentions the presence of any word of the 8 demographic identities; Black, White, Christian, Muslim, other religions, Male and Female. Therefore, the CivilComments dataset consists of 16 groups, formed by the combination of toxic labels and the presence or absence of the 8 demographic identities in each comment. Each demographic identity can potentially act as a spurious feature. To prevent this, the goal of the task is to train the model to focus solely on the invariant feature of toxic labels and not rely on demographic identities as predictive factors.

However, in reality, unlike other datasets, each comment in the CivilComments dataset can mention more than one demographic identity. Considering all possible combinations of demographic identities for each comment and training the model on all these combinations would be inefficient. Therefore, we follow the learning approach proposed by [19]. Concretely, we only consider four groups based on whether the comment mentions toxicity and whether it mentions the demographic identity of being “Black”, without considering other demographic identities. We train the model using these four groups. However, during the validation and test, we evaluate the model’s performance individually for all 16 groups and record the lowest accuracy among the group accuracies as the worst-group accuracy. The Best model is selected based on this worst-group accuracy.

A.5 Multi-NLI

Multi-NLI [38] is a task for classifying the entailment, neutrality, or contradiction between two sentences. According to [30], in the Multi-NLI dataset, the spurious feature is the negation word. Specifically, negation words, such as “No”, “Never”, “Nobody”, and “Nothing”, have a spurious correlation with the contradiction relationship between two sentences. This is the result of collecting more sentence examples with a contradiction relationship that includes negation words during the data collection process [25]. Therefore, we can obtain group accuracy for 6 groups based on the relationship between sentences and the presence of negation words. Our goal is to achieve the model with better worst-group accuracy. The training set, validation set, and test set all have the same group distribution. We select the best model based on the best worst-group accuracy on the validation set.

A.6 Experimental Details

We practically utilized the code provided in the PyTorch version⁴. The search range of the hyperparameter ρ , which determines the range for exploring the flat region, was fixed to $\{0.05, 0.2, 0.5, 0.8\}$ for all datasets. We evaluated the model using three random seeds and reported the average performance. For GDRO-related hyperparameters, we fix robust step size γ , in Algorithm 1 of the main paper, as 0.01. In addition, we use the same range for adjusted-group coefficient C , $\{0, 1, 2, 3\}$ (Section 3.3 in [30] for details), except for CMNIST and Multi-NLI. In CMNIST, Waterbirds and CelebA datasets, we utilize ResNet50 [14] models. The same hyperparameter ranges were applied ASAM and ASGDRO and the other performances for other baselines are reported performances from [25, 40, 13].

In CMNIST, we have the same hyperparameter search range as [40] by default: batch size 16, learning rate 10^{-3} , L2-regularization 10^{-4} with SGD over 300 epochs. For Waterbirds, we perform the grid search over the batch size, $\{16, 64\}$, the learning rate, $\{10^{-3}, 10^{-4}, 10^{-5}\}$, and L2-regularization, $\{10^{-4}, 10^{-1}, 1\}$. We train our model with SGD over 300 epochs. We also conduct grid search over the batch size, $\{16, 128\}$, the learning rate, $\{10^{-4}, 10^{-5}\}$, and L2-regularization, $\{10^{-4}, 10^{-2}, 1\}$ for CelebA, training with SGD over 50 epochs. We referenced [40, 25] for this range of hyperparameter search. For CivilComments, we use DistilBERT [31] model. We followed the hyperparameter search range provided in [19]. For optimizer, we use AdamW [27] with 10^{-2} for L2-regularization. We find the optimal learning rate among $\{10^{-6}, 2 \times 10^{-6}, 10^{-5}, 2 \times 10^{-5}\}$. We train up to 5 epochs with batch size 16. The gradient clipping was applied only during the second step, which is the actual update step, in the SAM-based algorithm [10]. The hyperparameter tuning range for Multi-NLI follows the setting of [25], except for the hyperparameter ρ . We train our model during 5 epochs and with an initial learning rate of 2×10^{-5} , batch size 32. We set the tokenization and dropout to its default value. We also do not use L2-regularization and adjusted-group coefficient C . We use AdamW [27] with clipping the gradient only for the second step.

B Heterogeneous-CMNIST (H-CMNIST): Experimental Details

In H-CMNIST experiments (Section 4.1 of the main paper), we use ResNet18 [14] with SGD. We also conduct reweighted sampling when the algorithm setting can use the group information, i.e., GDRO [30] and ASGDRO. For hyperparameter tuning, we perform grid search over learning rate, $\{10^{-3}, 10^{-4}\}$, and L2-regularization, $\{1, 10^{-1}, 10^{-3}, 10^{-4}\}$. We fix the batch size, 128, and train the model up to 20 epochs. For ASAM [21] and ASGDRO, we search the hyperparameter ρ among $\{0.05, 0.2, 0.5, 0.8\}$. We fix the robust step size, γ , as 0.01 for GDRO and ASGDRO.

C Grad-CAM Analysis

In this section, as an extension of Section 4.5 of the main paper, additional Grad-CAM [33] results on the Waterbirds and CelebA datasets are presented. In Figure 8 and 9, the red-colored-name features represent invariant features in the respective task, while the green-colored-name features represent spurious features. In the Grad-CAM images, the pixels that each model focuses on to predict the ground-truth label are highlighted closer to the red color in the image.

⁴<https://github.com/huaxiuyao/LISA>, <https://github.com/davda54/sam>

ERM [35] and ASAM [21] are regularization-free algorithms that do not specifically encourage models to focus on invariant features, and this is reflected in the Grad-CAM results. Specifically, when observing Group 0 and Group 3 of Waterbirds, which can strongly form the correlation between class and spurious, as well as Group 0, 1, and 2 of CelebA, in most cases, the results show a strong focus on both spurious and invariant features simultaneously or solely on spurious features. For some images, particularly between CelebA dataset’s Group 0 and 1 where there are no minority groups within a class, there is some degree of focus on invariant features. However, these images still contain a significant amount of unnecessary pixels such as the background. Conversely, in minority groups such as Group 1 and 2 in Waterbirds or Group 3 in CelebA, there is a predominant focus on invariant features to predict the ground-truth label. However, this focus is limited to only a subset of the overall invariant features and still include some spurious features.

In algorithms specifically designed to learn invariant features like GDRO [30], LISA [40], and ASGDRO (Ours), the Grad-CAM results exhibit different patterns compared to ERM and ASAM. In the most of results for the three algorithms, the models demonstrate a reasonable focus on invariant features. Compared with ERM and ASAM, there are significant reductions in the extent to which they focus on spurious features. However, GDRO and LISA still concentrate only on a part of invariant features. Additionally, in some cases, they may exhibit a greater focus on spurious features than on the subset of invariant features. It is also frequently observed that they still heavily include spurious features or solely focus on spurious features when dealing with majority groups such as Group 1 and 3 in Waterbirds or Group 0, 1, and 2 in CelebA. As we can see from the results of Group 1, and 2 in Waterbirds or Group 3 in CelebA, we can observe that the models’ low ability to fully concentrate on invariant features is affected by the performance of models that still exhibit a focus on spurious features. This observation highlights the impact of the models’ performance on their ability to completely focus on invariant features.

In contrast to other baselines, ASGDRO demonstrates a stronger focus on invariant features. As a result, Grad-CAM analysis shows that ASGDRO has relatively larger regions of focus on invariant features compared to other baselines. Simultaneously, it successfully eliminates spurious features while accurately predicting the ground-truth label. Therefore, these results demonstrate that ASGDRO has a higher capacity for capturing invariant features, and this characteristic is reflected in its performance. That is, ASGDRO guarantees that the model performs SIL.

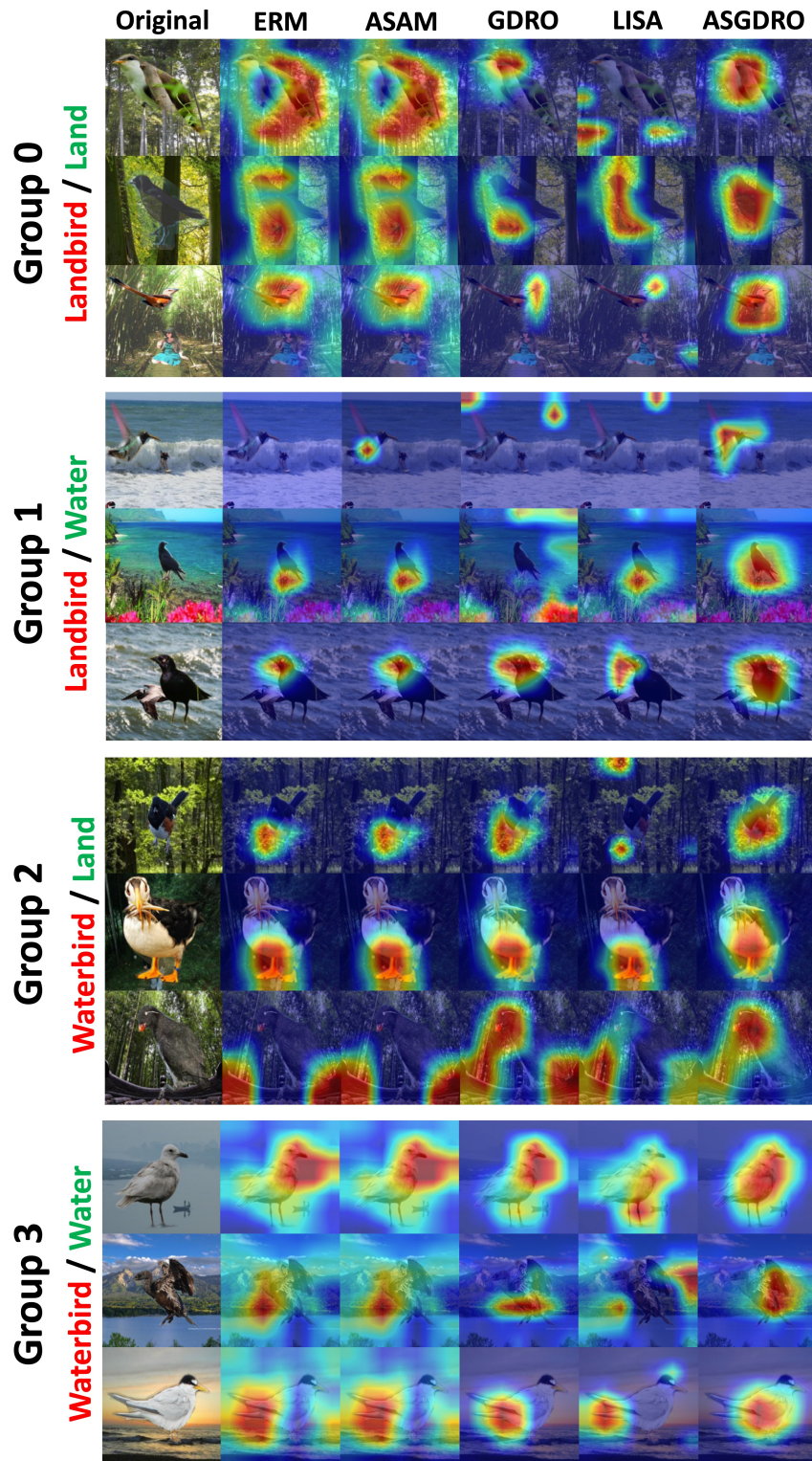


Figure 8: **Grad-CAM results on the Waterbirds Dataset.** The features highlighted in red represent invariant features: Landbird and Waterbird. On the contrary, the features highlighted in green represent spurious features: Land and Water background. In the Training Set, Group 1 and Group 2 are minority groups with significantly fewer data samples compared to other groups.

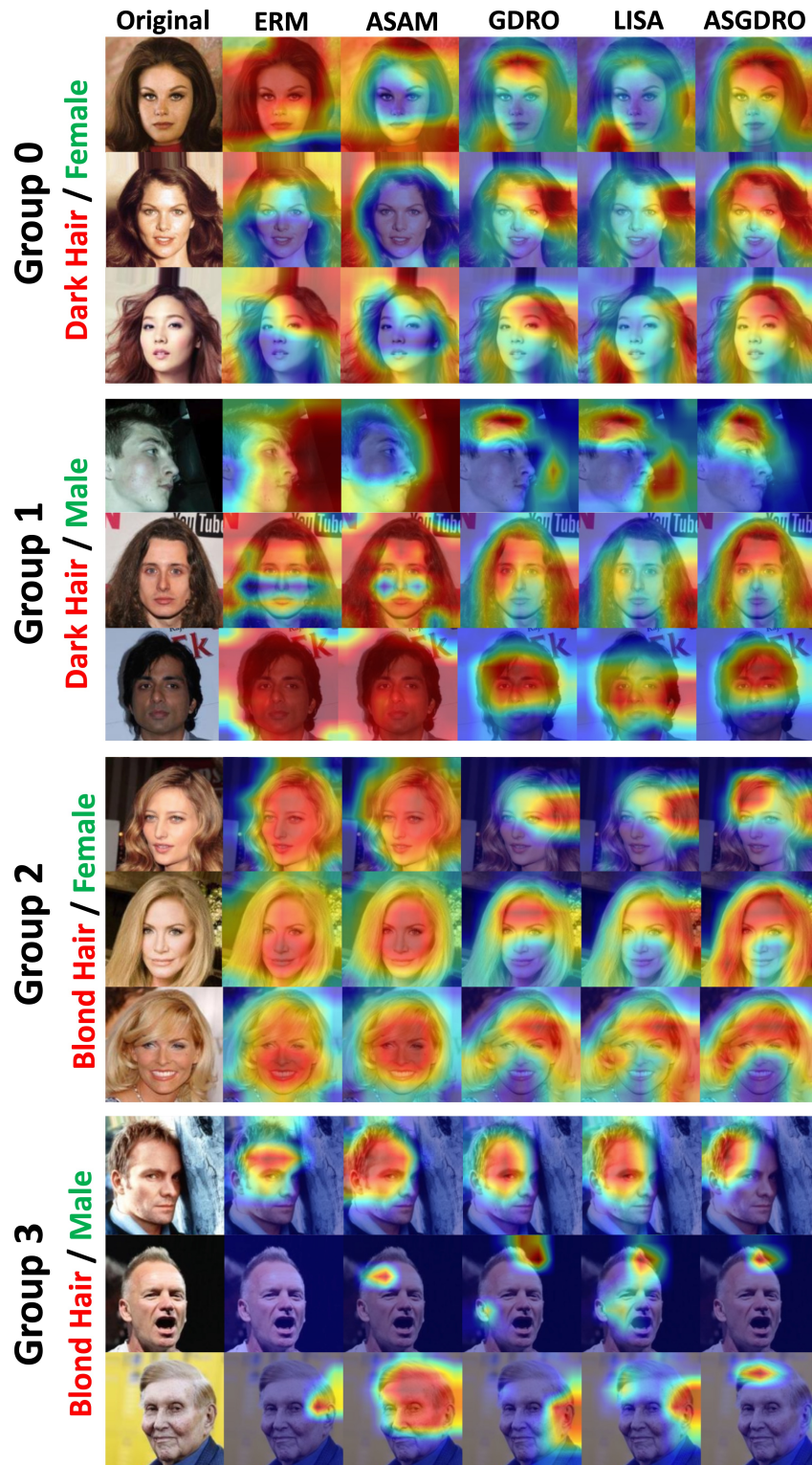


Figure 9: **Grad-CAM results on the CelebA Dataset.** The features highlighted in red represent invariant features: Dark Hair and Blond Hair. On the contrary, the features highlighted in green represent spurious features: Female and Male. In the Training Set, Group 3 is a minority group with significantly fewer data samples compared to other groups.

D Full DomainBed Results

Using DomainBed framework [12], we can evaluate Domain Generalization algorithms by randomly sampling hyperparameter combinations within predefined hyperparameter search ranges for each algorithm. The goal of Domain Generalization is to train models that perform robustly on unseen domains. Consequently, the choice of the best model is heavily influenced by whether the validation set used for model selection is sampled from the test domain or the train domains. To account for this, we provide results for both the training-domain validation set, which does not utilize information from the test domain, and the test-domain validation set, where model selection is performed using information from the test domain. The following subsections present the results for each dataset, considering both model selection methods.

By combining ASGDRO with the existing successful domain generalization approach, DPLCLIP [41]⁵, we demonstrate the versatility of ASGDRO, as it can easily be integrated with other algorithms. Moreover, our results show that ASGDRO not only improves performance in the context of subpopulation shift but also achieves performance gains in the presence of domain shift. For experimental details, we set the range of the robust step size γ as `lambda r: 10**r.uniform(-2, 0)` and the neighborhood size ρ as `lambda r: r.choice([0.05, 0.2, 0.5, 0.8])`. The other settings are the same as DPLCLIP [41]. Following common convention, we conducted 20 hyperparameter searches and reported the averages for three random seeds. We evaluated our model on the four datasets as in the original DPLCLIP paper: VLCS [23], PACS [9], OfficeHome [36], and TerraIncognita [3].

D.1 Model selection: training-domain validation set

D.1.1 VLCS

Algorithm	C	L	S	V	Avg
DPLCLIP	99.3 ± 0.3	61.9 ± 3.2	78.4 ± 1.0	83.4 ± 0.4	80.8
DPLCLIP GDRO	99.2 ± 0.3	66.3 ± 2.7	72.7 ± 0.9	82.7 ± 0.9	80.3
DPLCLIP ASGDRO	99.1 ± 0.6	65.6 ± 0.9	78.5 ± 0.8	85.4 ± 0.3	82.2

D.1.2 PACS

Algorithm	A	C	P	S	Avg
DPLCLIP	97.7 ± 0.1	96.4 ± 1.6	99.9 ± 0.0	90.4 ± 0.7	96.1
DPLCLIP GDRO	95.4 ± 1.4	97.9 ± 0.3	99.8 ± 0.1	89.6 ± 0.7	95.7
DPLCLIP ASGDRO	97.4 ± 0.5	98.6 ± 0.2	99.9 ± 0.0	90.5 ± 0.6	96.6

D.1.3 OfficeHome

Algorithm	A	C	P	R	Avg
DPLCLIP	79.5 ± 0.4	70.6 ± 0.8	88.8 ± 0.6	90.2 ± 0.3	82.3
DPLCLIP GDRO	80.6 ± 0.5	71.5 ± 0.8	89.6 ± 0.7	89.8 ± 0.3	82.9
DPLCLIP ASGDRO	80.5 ± 0.7	72.7 ± 0.4	89.8 ± 0.1	90.8 ± 0.3	83.5

D.1.4 TerraIncognita

Algorithm	L100	L38	L43	L46	Avg
DPLCLIP	39.2 ± 3.2	50.3 ± 1.7	44.6 ± 1.5	41.4 ± 1.0	43.9
DPLCLIP GDRO	38.6 ± 1.0	51.2 ± 1.5	44.5 ± 2.1	39.3 ± 2.8	43.4
DPLCLIP ASGDRO	46.7 ± 0.5	55.1 ± 0.6	46.0 ± 0.8	42.8 ± 2.1	47.6

⁵<https://github.com/shogi880/DPLCLIP>

D.1.5 Averages

Algorithm	VLCS	PACS	OfficeHome	TerraIncognita	Avg
DPLCLIP	80.8 ± 1.1	96.1 ± 0.2	82.3 ± 0.2	43.9 ± 1.2	75.8
DPLCLIP GDRO	80.3 ± 0.8	95.7 ± 0.3	82.9 ± 0.5	43.4 ± 1.3	75.6
DPLCLIP ASGDRO	82.2 ± 0.6	96.6 ± 0.3	83.5 ± 0.1	47.6 ± 0.8	77.5

D.2 Model selection: test-domain validation set (Oracle)

D.2.1 VLCS

Algorithm	C	L	S	V	Avg
DPLCLIP	99.8 ± 0.1	69.4 ± 0.8	78.6 ± 1.2	86.2 ± 0.6	83.5
DPLCLIP GDRO	99.5 ± 0.2	69.3 ± 1.6	77.1 ± 1.0	86.4 ± 0.5	83.1
DPLCLIP ASGDRO	99.8 ± 0.1	69.7 ± 1.1	80.5 ± 0.6	86.1 ± 0.4	84.0

D.2.2 PACS

Algorithm	A	C	P	S	Avg
DPLCLIP	97.5 ± 0.2	98.5 ± 0.2	99.6 ± 0.2	92.1 ± 0.2	96.9
DPLCLIP GDRO	97.9 ± 0.1	98.4 ± 0.2	99.7 ± 0.1	91.7 ± 0.6	96.9
DPLCLIP ASGDRO	97.9 ± 0.0	98.8 ± 0.1	99.9 ± 0.0	92.1 ± 0.4	97.2

D.2.3 OfficeHome

Algorithm	A	C	P	R	Avg
DPLCLIP	80.3 ± 0.5	72.4 ± 0.3	89.9 ± 0.2	90.5 ± 0.1	83.3
DPLCLIP GDRO	80.6 ± 0.9	72.7 ± 0.4	89.7 ± 0.5	90.8 ± 0.2	83.5
DPLCLIP ASGDRO	80.8 ± 0.1	72.7 ± 0.2	90.0 ± 0.3	90.5 ± 0.3	83.5

D.2.4 TerraIncognita

Algorithm	L100	L38	L43	L46	Avg
DPLCLIP	57.1 ± 2.8	57.3 ± 0.5	47.6 ± 1.6	48.5 ± 1.3	52.6
DPLCLIP GDRO	56.4 ± 1.3	55.8 ± 1.1	47.8 ± 1.5	41.4 ± 0.2	50.4
DPLCLIP ASGDRO	57.3 ± 1.3	57.4 ± 0.4	50.4 ± 1.3	43.6 ± 1.3	52.2

D.2.5 Averages

Algorithm	VLCS	PACS	OfficeHome	TerraIncognita	Avg
DPLCLIP	83.5 ± 0.2	96.9 ± 0.1	83.3 ± 0.0	52.6 ± 0.4	79.1
DPLCLIP GDRO	83.1 ± 0.8	96.9 ± 0.1	83.5 ± 0.2	50.4 ± 0.5	78.5
DPLCLIP ASGDRO	84.0 ± 0.5	97.2 ± 0.1	83.5 ± 0.0	52.2 ± 0.3	79.2